CHINESE JOURNAL OF PHYSICS VOL. 33, NO. 3 JUNE 1995

Six-Wave Mixing Near-Infrared Emissions in Rubidium Vapor

Yao-Ju Chan and Wei-Tzou Luh

Department of Chemistry, National Chung Hsing University, Taichung, Taiwan 402, R.O.C.

(Received March 3, 1995; revised manuscript received March 30, 1995)

During two-photon excitation studies of rubidium vapor, in addition to Rb near-infrared atomic transitions, we have observed several stimulated near-infrared emissions. For the $5S$-$5D$ two-photon allowed excitation we observed emissions near 1.325, 1.369, 1.373, 1.477, 1.533 and 1.537 μm, and for the Rb $5S$-$7S$ two-photon allowed excitation we observed emissions near 1.330, 1.395, 1.432, 1.484, 1.564 and 1.613 μm. The eight emissions, near 1.325, 1.330, 1.369, 1.395, 1.477, 1.484, 1.533 and 1.564 μm are interpreted as axially phase-matched six-wave mixing emissions, while the other four emissions, near 1.373, 1.432, 1.537 and 1.613 μm, are interpreted as angle phase-matched six-wave mixing emissions. Temperature (or number density)-dependent evolution curves of some of the above six-wave mixing emissions have also been measured. The results reveal that different mixing processes occur at different rubidium number densities.

PACS. 42.65.Ky – Harmonic generation, frequency conversion, parametric oscillation, and parametric amplification.

I. INTRODUCTION

When alkali metal vapors are excited by high-power pulsed lasers tuned near the two-photon allowed atomic transitions, both angle [1-12] and axially phase-matched wave-mixing emissions [9,13-17] can be generated. For the axial and angle phase-matched processes, both photon energy conservation ($2\omega_L = \Sigma_i \omega_i$, where ω_L is the angular frequency for the pumping laser photon and ω_i for the photon i involved in the cascading channel) and photon momentum conservation ($2k_L = \Sigma_i k_i$, where k_L is the wave vector for the pumping laser photon and $\vec{k}_i$ for the photon i) must be simultaneously satisfied. For the axially phase-matched process, the photons all propagate in the same direction, so photon momentum conservation reduces to a relation among the magnitudes ($2|\vec{k}_L| = \Sigma_i |\vec{k}_i|$). So far, angle phase-matched wave-mixing processes have been most often observed. Recently, however the axially phase-matched wave-mixing process has been theoretically and experimentally

investigated by Moore et al. [13]. Most of the previous studies were mainly interested in the generation of coherent UV radiation, but some recent studies have begun considering schemes for the generation of coherent near-infrared radiation [8-10,14-16].

In 1989, Luh et al. [14] demonstrated, both experimentally and theoretically, that the intriguing 830 nm coherent emission [6,18-20], which was observed when sodium vapor was pumped with a high-power pulsed laser tuned near the $3S$-$4D$ two-photon allowed transition, was actually an axially phase-matched six-wave mixing (ASWM) emission rather than an excimer-like $Na_2 1^3\Sigma_g^+ - 1^3\Sigma_u^+$ bound-free emission as had been previously suggested [18]. This ASWM process (designated as the DKS-type below, from the initials of Dinev et *al.* [19] who first observed the 830 nm emission in sodium vapor) obeyed the two conditions [14]:

$$\omega_{830\ \mathrm{nm}} = 2\omega_L - \omega_{4D-4P} - \omega_{4P-3D} - \omega_{584\ \mathrm{nm}}, \tag{1}$$

and

$$|\vec{k}_{830\ \mathrm{nm}}| = 2|\vec{k}_L| - |4D - 4P| - |\vec{k}_{4P-3D}| - |\vec{k}_{584\ \mathrm{nm}}|. \tag{2}$$

Note that in the DKS-type ASWM process, the idler photon $\omega_{584\ \mathrm{nm}}$ occurred at peculiarly large detunings of about 150 cm-' from the atomic D1 and D2 lines (589 nm and 589.6 nm), while the other ASWM process observed by Moore et al. [13] (designated as the MGP-type) at 818.46 nm, obeyed the two conditions:

$$\omega_{818.46\ \mathrm{nm}} = 2\omega_L - \omega_{4D-4P} - \omega_{4P-3D} - \omega_{589.52\ \mathrm{nm}}, \tag{3}$$

and

$$|\vec{k}_{818.46\ \mathrm{nm}}| = 2|\vec{k}_L| - |\vec{k}_{4D-4P}| - |\vec{k}_{4P-3D}| - |\vec{k}_{589.52\ \mathrm{nm}}|. \tag{4}$$

In this MGP-type process, the corresponding idler photon $\omega_{589.52\ \mathrm{nm}}$, whose wavelength was calculated from the energy conservation Eq. (3), is located between the atomic D1 and D2 lines (see also the inset of Fig. 4 in Ref. [13]). Since these two processes are not quite the same, more theoretical and experimental work with other alkali vapors seemed desirable in order to gain additional insight. Luh [15] then calculated several possible DKS-type ASWM wavelengths in pure and mixed alkali vapors. In potassium vapor, Jabbour et al. [9] observed MGP-type ASWM emissions at 1.172~ and 1.246~ during their study on broadly tunable near-infrared six-wave mixing processes produced using the K $4S$-$6S$ two-step excitation. Recently Lu and Liu [16] observed both MGP-type and DKS-type ASWM emissions using an IR up-conversion technique during their systematic study of axially phase-matched parametric four- and six-wave mixing processes produced using the K $4S$-$6S$ twophoton excitation. Lu and Liu also noted that the DKS-type emissions at

1.22μ and 1.30μ were detectable if the dye laser used in the two-photon excitation was operated with the dye LDS751, but were not detectable if the dye LDS698 was used. Since the intensity of the amplified spontaneous emission (ASE) at 749 nm generated by the dye LDS 751 was found to be 100 times higher than that generated by the dye LDS698 (see Fig. 8 of Ref. [16]), they argued that the ASE at 749 nm took part as one of the idler photons involved in the wave-mixing process. In a subsequent work, Lu and Liu [17] found that the intensity of the Na DKS-type 830 nm and 1.16μ emissions was dramatically reduced if the ASE emission at 584 nm of the R590 dye was mostly eliminated by a band-pass filter, and provided additional evidence to support their earlier argument that the ASE of a dye laser took part in the DKS-type mixing process.

In a continuous effort, aimed at confirming part of our previous predictions [15] and at comparing different mixing or excitation channels, we have investigated near-infrared six-wave mixing emissions in rubidium vapor which is pumped by a pulsed dye laser tuned near the rubidium $5S$-$5D$ or $5S$-$7S$ two-photon allowed transitions. Note that Korolev et al. [21] investigated these two systems and reported a series of stimulated infrared atomic transitions and two violet parametric emissions, but they did not report any of the type of six-wave mixing near-infrared parametric emissions that we mentioned above. It is interesting to note that the wavelengths of the pump lasers for the $5S$-$5D$ and $5S$-$7S$ two-photon allowed transitions and the wavelengths of the involved ASE idler photons are all located within the tunable lasing spectral range of the laser dye LDS759. One may investigate these two excitation channels with a single dye. If the argument of Lu and Liu is operative, then one may use this advantage to observe the axially phase-matched mixing emissions previously predicted in rubidium vapor. Indeed we have observed all these predicted DKS-type emissions. Fig. 1 presents a partial energy level diagram of the rubidium atom showing (a) the two angle phase-matched six-wave mixing processes, (b) the two axially phase-matched six-wave mixing processes of the MGP-type and (c) two of the DKS-type observed during the rubidium $5S$-$5D$ two-photon allowed excitation. In the following, Sec. I describes experimental details, Sec. II presents the results and discussion and Sec. III presents our conclusions.

II. EXPERIMENT

Figure 2 shows schematically the experimental setup. A Nd:YAG laser (Lumonics YM600), operated at a repetition rate of 10 Hz and adjusted to have a pulse energy of $\sim$ 50 mJ at 532 nm, was used to pump a dye laser (Lumonics HD-500). The dye laser, operated with the dye LDS759, produced an output energy of $\sim$ 1.0 mJ at 760 nm and $\sim$ 0.5 mJ

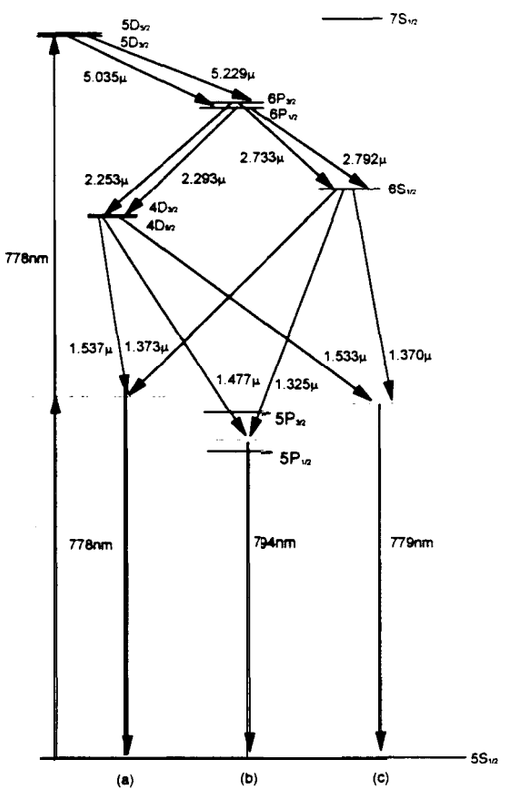

FIG. 1. A partial energy level diagram of the rubidium atom; (a) angle phase-matched six-wave mixing channels, (b) axially phase-matched six-wave mixing channels of the MGP-type, and (c) axially phase-matched six-wave mixing channels of the DKS-type.

at 778 nm, with a pulse duration of $\sim$ 6 ns and a linewidth of $\sim$ 0.04 cm-‘ .

A 50 cm long linear heat-pipe oven containing pure rubidium metal was used for the present work but it was not operated in the heat-pipe mode. The oven had a 20 cm long heating zone, and the temperature was typically varied in the 400 K - 650 K range, corresponding to a rubidium vapor pressure range of 1.6 x 10^{-3} - 11 mbar [22] and in turn to an atom number density range of 2.9 x $10^{13}\,cm^{-3}$ - 1.3 x $10^{17}\,cm^{-3}$. Gaseous argon was used as a buffer.

The pump laser beam was aligned through the center of the heat-pipe oven and directed onto the entrance slit of a 0.5 m monochromator (Acton SP-500), in which forward (along the direction of the laser beam) stimulated emissions and wave-mixing emissions from

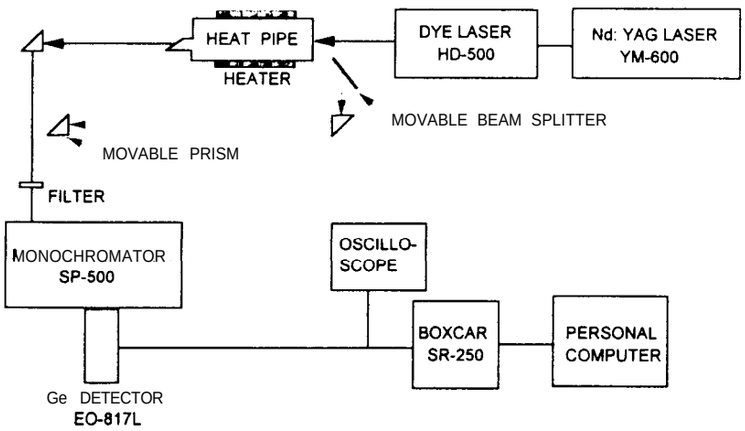

FIG. 2. Schematic of the experimental setup.

the excited rubidium vapor were resolved. A movable beam splitter before the entrance window of the heat-pipe oven was occasionally used to observe backward (opposite to the direction of the laser beam) emissions in order to identify parametric emissions. However only the forward results will be presented below. Note that although we did not employ an adjustable aperture and a focusing lens to distinguish the angle and the axially phase-matched emissions as before [14], their spectral locations are confined by the energy and momentum conservation conditions and can be well predicted. The entrance and exit slit widths of the monochromator were typically set at 50μ. Each resolved near-infrared emission was detected by a liquid-nitrogen cooled germanium detector (North Coast EO817L), which had a sensitive spectral range of $0.8\text{-}1.7\mu$ with a maximum sensitivity near 1.55~. The ac output from the detector was averaged by a gated boxcar-averager (SRS SR250) and then recorded by a personal computer for later analysis.

Argon and krypton pen lamps (Oriel) were used for wavelength calibration. The wavelength uncertainty for each emission peak was f0.2 nm. A sodium-potassium (Na-K) hollow cathode lamp (Perkin Elmer) filled with neon gas and a chromium (Cr) hollow cathode lamp (Hitachi) filled with argon gas were used to calibrate the laser wavelength by using optogalvanic spectroscopy; the resultant uncertainty for laser wavelength was fO.O1 nm. For the relative measurements of laser power and ASE emission intensity, the laser beam was directed onto a white disperser before the monochromator and then detected by a photomultiplier (EMI9863QB).

For emission spectra, we set the pump laser at a particular wavelength and scanned the monochromator. For temperature-dependent measurements, we set the monochromator at a particular six-wave mixing wavelength and the pump laser at a particular pump wavelength. We then started heating the heat-pipe oven, and simultaneously recorded the variation of the wall temperature at the center of the heat-pipe oven and the intensity evolution of this particular wave mixing emission.

III. RESULTS AND DISCUSSION

In the following, we present and discuss the near-infrared emissions obtained using the Rb $5S$-$5D$ two-photon allowed excitation in Sec. III-l, in Sec. III-2 those using the $5S$-$7S$ two-photon allowed excitation, and then in Sec. III-3 the temperature evolution curves of some six-wave mixing emissions.

III-l. The Rb $5S$-$5D$ two-photon excitation

One of several observed emission spectra is presented in Fig. 3. Here the wavelength of the dye laser was tuned to a particular wavelength, 777.85 nm, near the wavelength for the resonant Rb $5^2S_{1/2}$-$5^2D_{3/2,5/2}$ two-photon allowed transition [21,23]. We observed ten near-infrared emission peaks located at 1.3235, 1.3250, 1.3664, 1.3697, 1.3732, 1.4751, 1.4768, 1.5289, 1.5330 and 1.5373 μm, respectively. The two sharp emission peaks at 1.3235~ and 1.3664μ, shown in Fig. 3(a) and (b), correspond to the $5^2P_{1/2,3/2}$-$6^2S_{1/2}$ allowed transitions and those at 1.4751~ and 1.5289μ, in Fig. 3(c) and (d), correspond to the $5^2P_{1/2,3/2}$-$4^2D_{3/2,5/2}$ allowed transitions. All other emission peaks are summarized in Table I and they can be attributed to the parametric wave-mixing processes described below.

The relatively strong 1.3732~ and 1.5373~ emission peaks, in Fig. 3(b) and (d), can each be interpreted as an angle phase-matched six-wave mixing process via the $6S$ and $4D$ intermediate state, respectively (see also Fig. 1 (a)), according to the two conditions [6]:

$$\omega_{1.3732(\ 1.5373)} = 2\omega_{777.85\ \mathrm{nm}} - \omega_{5D-6P} - \omega_{6P-6S(4D)} - \omega_{777.85\ \mathrm{nm}}, \tag{5}$$

and

$$k_{1.3732(\ 1.5373)} = 2k_{777.85\ \mathrm{nm}} - k_{5D-6P} - k_{6P-6S(4D)} - \vec{k}_{777.85\ \mathrm{nm}}. \tag{6}$$

Note that during this angle phase-matched wave-mixing process, the laser beam of 777.85 nm provides not only the exciting photons for the Rb $5S$-$5D$ two-photon allowed transition but also the idler photons for the wave-mixing processes.

The relatively weak and broad 1.3250μ and 1.4768~ emission peaks, in Fig. 3(a) and (c), can each be attributed to an MGP-type emission [13], resulting from an axially phase-matched six-wave mixing process via the $6S$ and $4D$ intermediate states, respectively

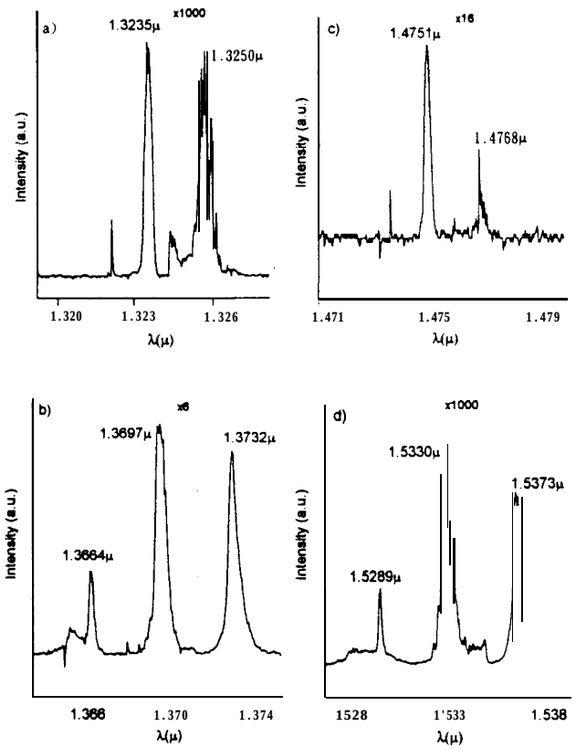

FIG. 3. Observed emission spectra due to excitation near the $5S$-$5D$ two-photon allowed transition at 777.85 nm. The heat-pipe oven was operated at a temperature of 538 K, corresponding to a Rb number density of 8.9 x $10^{15}\,\mathrm{cm}^{-3}$, and an argon gas pressure of 17.5 mbar.

(see also Fig. 1 (b)), according to the two conditions:

$$\omega_{1.3250(1.4768)} = 2\omega_{777.85\ \mathrm{nm}} - \omega_{5D-6P} - \omega_{6P-6S(4D)} - \omega_{794\ \mathrm{nm}}, \tag{7}$$

and

$$|\vec{k}_{1.3250(1.4768)}| = 2|\vec{k}_{777.85\ \mathrm{nm}}| - |\vec{k}_{5D-6P}| - |\vec{k}_{6P-6S(4D)}| - |\vec{k}_{794\ \mathrm{nm}}|. \tag{8}$$

These two observed spectral wavelengths are consistent with the theoretical phase-matched spectral wavelengths, which have been calculated using (3) and (4) and the Sellmeir equation, as was done previously in the case of the sodium 830 nm emission [14]. Some required Rb atomic transition frequencies and oscillator strengths have been taken from the literature [24,25].

The moderate and broad 1.3697μ and 1.5330~ emission peaks, in Figs. 3(b) and (d),

TABLE I. Observed six-wave mixing near-infrared emissions in rubidium vapor. λ_{exc} describes the wavelength of the pumping laser beam; $2-h\nu$ describes the pumped twophoton allowed Rb atomic transition; the third and fourth columns present the observed six-wave near-infrared emissions via the Rb $6S$; and $4D$ intermediate states, respectively; and the fifth column classifies each observed emission, as detailed in the text. The uncertainty is ± 0.01 nm for the laser wavelength, and $\pm 0.0002\mu$ for each observed emission wavelength.

		$\lambda_{obs}(\mu)$		
λ_{exc} (nm)	$2-h\nu$	$6S$ channel	$4D$ channel	Type
777.85	$5S$-$5D$	1.3250	1.4768	MGP
		1.3697	1.5330	DKS
		1.3732	1.5373	Angle
759.93	$5S$-$7S$	1.3302	1.4835	MGP
		1.3948	1.5647	DKS
		1.4327	1.6127	Angle

are the two DKS-type emissions that we are looking for [15]. Each results from an axially phase-matched six-wave mixing process via the $6S$ and $4D$ intermediate states, respectively (see also Fig. 1 (c)), according to the two conditions:

$$\omega_{1.3697(1.5330)} = 2\omega_{777.85\text{nm}} - \omega_{5D-6P} - \omega_{6P-6S(4D)} - \omega_{779\text{ nm}}, \tag{9}$$

and

$$|\vec{k}_{1.3697(1.5330)}| = 2|\vec{k}_{777.85\text{ nm}}| - |\vec{k}_{5D-6P}| - |\vec{k}_{6P-6S(4D)}| - |\vec{k}_{779\text{ nm}}|. \tag{10}$$

In (7) through (10) 779 nm and 794 nm were the calculated wavelengths. For visibility, the relative intensities of the stronger emission peaks in Fig. 3 were intentionally reduced by using neutral density filters. In Fig. 3(a), the number $\times 1000$ means that the intensity scale for the 1.3250~ emission peak is in fact only one thousandth of that for the 1.3235~ emission peak. Note that the relative intensities of the emission peaks varied as the wavelength of the exciting laser beam was changed, as is demonstrated in Fig. 4(a). The dependence upon the number density of rubidium atoms (the temperature of the heat-pipe oven) is demonstrated in Fig. 4(b), in which the intensity of the 1.3697μ emission peak increases as the oven temperature increases and then drops again at higher Rb number densities, but

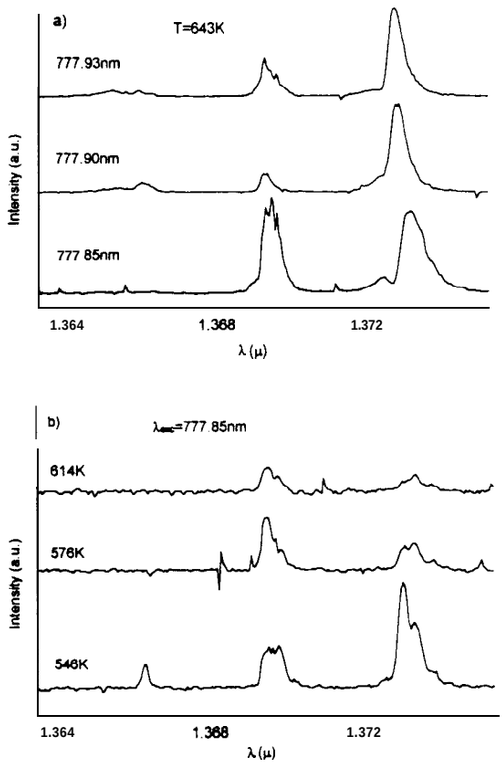

FIG. 4. Variation in the relative intensities of the 1.3697μ and 1.3732~ lines upon (a) a change of wavelength of the pump laser at 643 K and under 18.7 mbar of argon, and (b) a change in the oven temperature at 777.85 nm and under 19.2 mbar of argon. Note that the vertical scale for (a) is in fact one hundredth of that for (b).

the intensity of the **1.3732~** emission peak always deceases. We did not explore this further due to their dependence on the wavelength of the exciting laser beam as shown above in Fig. 4(a). Note that the intensity scale in Fig. 4(a) is actually only one hundredth of that in Fig. 4(b).

111-2. The Rb $5S$-$7S$ two-photon excitation

Figure 5 presents one of several observed emission spectra. The wavelength of the dye laser was tuned to 759.93 nm, near the resonant Rb $5^2S_{1/2}-7^2S_{1/2}$ two-photon allowed transition wavelength 759.916 nm. Under these conditions we observed several near-infrared emission peaks located at 1.3235, 1.3302, 1.3664, 1.3948, 1.4327, 1.4751, 1.4835, 1.5289,

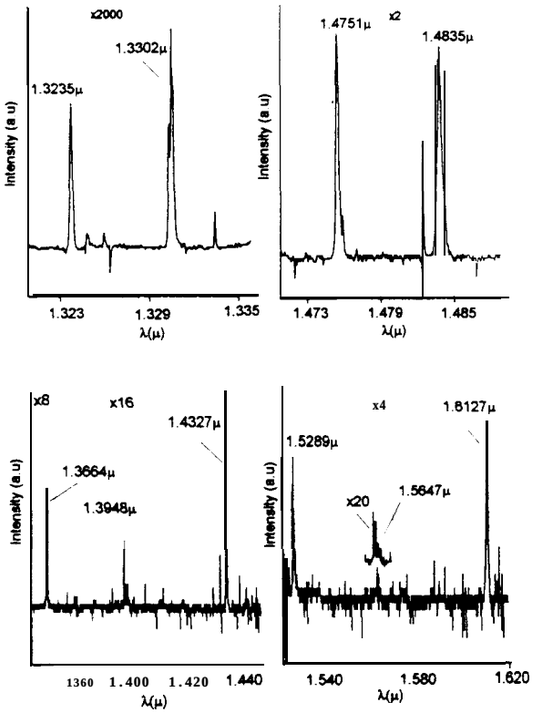

FIG. 5. Observed emission spectra due to the near $5S$-$7S$ two-photon allowed excitation at 759.93 nm. The heat-pipe oven was operated at 604 K, corresponding to 5.5 x $10^{16}\,\mathrm{cm}^{-3}$ of Rb atoms, and under an argon gas of 17.6 mbar.

1.5647 and 1.6127 μm, respectively. The sharp emission peaks at 1.3235~ and 1.3664~ are due to the $5^2P_{1/2,3/2} - 6^2S_{1/2}$ allowed transitions and those at 1.4751~ and 1.5289μ are due to the $5^2P_{1/2,3/2} - 4^2D_{3/2,5/2}$ allowed transitions. All other emission peaks are summarized in Table I and can be attributed to parametric wave-mixing processes similar to the Rb $5S$-$5D$ pumping case. The weak 1.3302~ and 1.4835~ emission peaks are each an MGP-type emission, via the respective $6S$ and $4D$ intermediate states, with an idler photon near 792 nm. The relatively broad 1.3948μ and 1.5647~ emission peaks are each of the DKS-type emission that we are seeking, via the respective $6S$ and $4D$ intermediate states, with an idler photon of near 771 nm. Note that although the spectral peak at 1.5647~ may not have a very high signal/noise ratio to justify itself, as shown in Fig. 5, its actual intentsity varies as the wavelength of the dye laser detunes or the density of rubidium atoms changes [26], (see also Fig. 4 for the Rb $5S$-$5D$ case). The strong 1.4327~ and 1.6127~ emission peaks are each due to an angle phase-matched six-wave mixing process, via the respective $6S$ and

$4D$ intermediate states, having an additional laser photon involved as an idler photon. Note that as discussed below, the DKS-type axially phase-matched emissions from the Rb $5S$-$7S$ excitation could only be observed at higher number densities for rubidium atoms than the analogous emissions produced with the $5S$-$5D$ pumping, although the exciting laser beam at 760 nm had twice the pulse energy as at 778 nm.

III-3. Evolution curves

In order to reveal the differences between different wave-mixing channels, the intensities of several six-wave mixing emissions were monitored as the number density of the rubidium atoms (the temperature of the heat-pipe oven) was increased. Fig. 6 presents the evolution curves of two axially phase-matched emissions, at 1.3697μ and 1.5330μ, and two angle phase-matched emissions, at 1.3732μ and 1.5373μ, due to the $5S$-$5D$ two-photon excitation at 777.85 nm. Fig. 7 presents the evolution curves of one axially phase-matched emission at 1.3949μ and one angle phase-matched emission at 1.4329μ due to the $5S$-$7S$ two-photon excitation at 759.86 nm. Note that these evolution curves were obtained with only a long-pass filter placed between the heat-pipe oven and the monochromator, and that the measurements were stopped shortly after the noticeable emission intensity and a discernible onset temperature for the wave-mixing process could be seen.

One can tell from Fig. 6 that angle phase-matched six-wave mixing processes start to occur at lower rubidium densities than axially phase-matched six-wave mixing processes do, and that either angle or axially phase-matched wave-mixing processes through the $6S$ intermediate state occur at lower densities than the corresponding mixing processes through the $4D$ intermediate state. One can also tell, by comparing Fig. 6 with Fig. 7, that the six-wave mixing processes produced by $5S$-$7S$ pumping can only occur at higher Rb number densities than those produced by $5S$-$5D$ pumping. For a more quantitative analysis of these evolution curves, substantial calculations on the fifth-order susceptibilities $\chi^{(5)}$ of the nonlinear processes, such as Pong [27] did for the sodium sytem, are strongly desirable. We will collaborate with the Yih group at National Central University and publish these results in another paper later on.

IV. CONCLUSIONS

We observed several six-wave mixing near-infrared emissions in rubidium vapor when the dye laser was tuned near the Rb $5S$-$5D$ or $5S$-$7S$ two-photon allowed transition and confirmed our previous predictions on axially phase-matched six-wave mixing emissions [15]. Here we have performed experiments to observe the DKS-type emissions by using a dye following the argument of Lu and Liu [16,17].

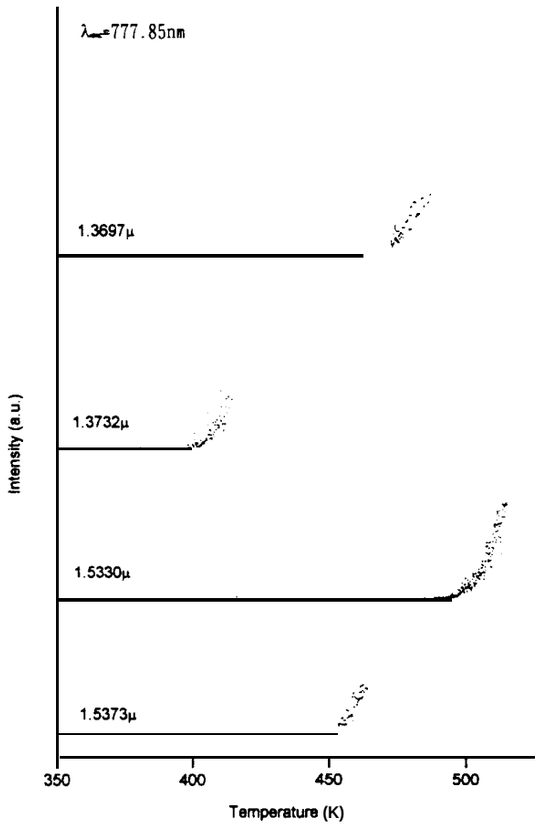

FIG. 6. Evolution curves of two angle phase-matched six-wave mixing emissions, 1.3732~ and 1.5373μ, and of two axially phase-matched six-wave mixing emissions, 1.3697μ and 1.5330μ, produced by laser pumping near the $5S$-$5D$ two-photon transition at 777.85 nm. The argon buffer gas pressure was 17.6 mbar.

The temperature-dependent evolution curves of these emissions have also been measured. The results reveal that the angle phase-matched six-wave mixing processes occur at rubidium number densities which are lower than those where the axially phase-matched processes are observed, that either angle or axially phase-matched six-wave mixing processes involving the $6S$ state in the downward emission cascade occur at densities lower than the corresponding processes involving the $4D$ level, and that either angle or axially phase-matched six-wave mixing processes produced when pumping the $5S$-$5D$ two-photon allowed transition occured at lower densities than the corresponding emission produced

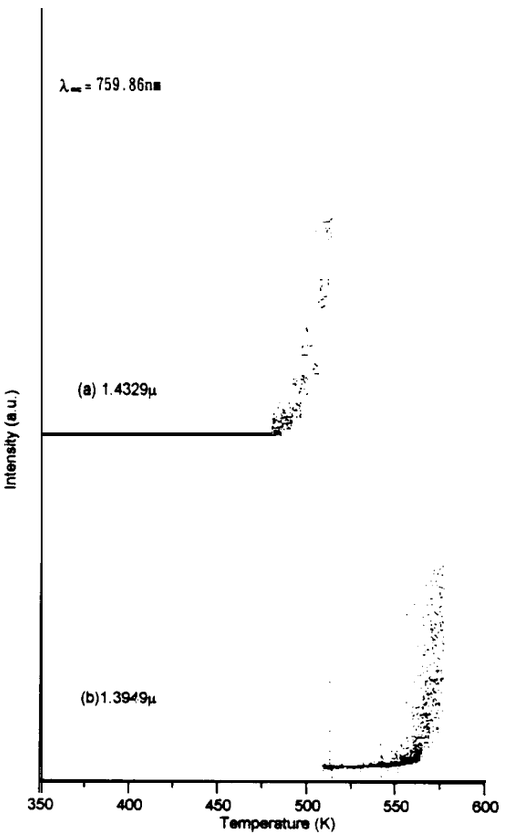

FIG. 7 Evolution curves of one axially phase-matched six-wave mixing emission at 1.3949μ and one angle phase-matched six-wave mixing emission at 1.4329μ, due to laser pumping near the $5S$-$7S$ two-photon transition at 759.86 nm. The argon buffer gas pressure was 17.6 mbar.

from $5S$-$7S$ two-photon allowed excitation. Theoretical calculations on the fifth-order susceptibilities involved in nonlinear processes are strongly desirable for a more rigorous and quantitative treatment of these evolution curves.

ACKNOWLEDGMENTS

This work was in part supported by the National Science Council under grant (NSC83-0208-M-005-036). We thank Professor John P. Huennekens for his valuable comments and the referee for their helpful suggestions.

REFERENCES

[1] D. Cotter, D. C. Hanna, W. H. W. Tuttlebee, and M. A. Yuratich, Opt. Commun. 22, 190 (1977).

[2] W. Hartig, Appl. Phys. 15, 427 (1978).

[3] P. L. Zhang, Y. C. Wang, and A. L. Schawlow, J. Opt. Soc. Am. **B1, 9** (1984).

[4] J. Karsinski, D. J. Gauthier, M. S. Malcuit, and R. W. Boyd, Opt. Commun. 54, 241 (1985).

[5] S. M. Hamadani, J. A. D. Stockdale, R. N. Compton, and M. S. Pindzola, Phys. Rev. A34, 1938 (1986).

[6] Z. G. Wang, H. Schmidt, and B. Wellegehausen, Appl. Phys. B44, 41 (1987).

[7] M. A. Moore, W. R. Garrett, and M. G. Payne, Opt. Commun. 68, 310 (1988).

[8] B. K. Clark, M. Masters, and J. Huennekens, Appl. Phys. B47, 159 (1988).

[9] Z. J. Jabbour, M. S. Malcuit, and J. Huennekens, Appl. Phys. B52, 281 (1991).

[10] H. S. Fung, T. E. Nee, P. J. Tsai, W. T. Cheng, H. H. Wu, T. S. Yih, Chin. J. Phys. (Taipei) 31, 265 (1993).

[11] F. Z. Chen, X. F. Han, and C. Y. R. Wu, Appl. Phys. B56, 113 (1993).

[12] T. S. Yih, H. H. Wu, H. S. Fung, J. E. Fan, B. J. Pong, C. Y. R. Wu, Chin. J. Phys. (Taipei) 31, 497 (1993).

[13] M. A. Moore, W. R. Garrett, and M. G. Payne, Phys. Rev. **A39, 3692** (1989).

[14] W. T. Luh, Y. Li, and J. Huennekens, Appl. Phys. B49, 349 (1989).

[15] W. T. Luh, Chin. J. Phys. (Taipei) 28, 139 (1990). Note that there are two errors for the Rb $5S$-$7S$ case in Table I, $4S$-$7S$ and 1364.69 are corrected as $5S$-$7S$ and 1394.69, respectively.

[16] Mao-hong Lu and Yu-mei Liu, Appl. Phys. B54, 288 (1992).

[17] Yu-mei Liu and Mao-hong Lu, Chin. J. Phys. (Taipei) 31, 105 (1993).

[18] D. D. Konowalow and P. S. Juliene, J. Chem. Phys. 72, 5815 (1980).

[19] S. G. Dinev, I. G. Koprinkov, and I. L. Stefanov, Opt. Commun. **52,** 199 (1984).

[20] S. J. Bijic, R. N. Compton, J. A. D. Stockdale, and D. D. Konowalow, J. Chem. Phys. 89, 7056 (1988).

[21] F. A. Korolev, V. V. Martynov, V. I. Odintsov, and A. 0. Fakhmi, Opt. Spectrosc. 40, 600 (1976).

[22] A. G. Mozgovoi, I. I. Novikov, M. A. Pokrasin, and V. V. Roschupkin, High Temp-High Pressure 19, 425 (1987).

[23] A. M. Bench-Bruevich, V. A. Khodovoi, and V. V. Khromov, JETP Lett. 14, 333 (1971).

[24] C. E. Moore, Atomic *Energy Levels,* Vol. II, NSRDS-NBS 35 (1971).

[25] E. Caliebe and K. Niemax, J. Phys. B12, L45 (1979).

[26] Y. J. Chan, M. S. Thesis, National Chung Hsing University, June, 1994.

[27] B. J. Pong, Ph. D. Thesis, National Central University, June, 1994.